Regularly timed events amid chaos

Jonathan N. Blakely, Roy M. Cooper, and Ned J. Corron
Charles M. Bowden Laboratory, U.S. Army Aviation and Missile Research, Development and Engineering Center, RDMR-WDS-WR, Redstone Arsenal, Alabama 35898, USA
(Received 28 July 2015; published 6 November 2015)

We show rigorously that the solutions of a class of chaotic oscillators are characterized by regularly timed events in which the derivative of the solution is instantaneously zero. The perfect regularity of these events is in stark contrast with the well-known unpredictability of chaos. We explore some consequences of these regularly timed events through experiments using chaotic electronic circuits. First, we show that a feedback loop can be implemented to phase lock the regularly timed events to a periodic external signal. In this arrangement the external signal regulates the timing of the chaotic signal but does not strictly lock its phase. That is, phase slips of the chaotic oscillation persist without disturbing timing of the regular events. Second, we couple the regularly timed events of one chaotic oscillator to those of another. A state of synchronization is observed where the oscillators exhibit synchronized regular events while their chaotic amplitudes and phases evolve independently. Finally, we add additional coupling to synchronize the amplitudes, as well, however in the opposite direction illustrating the independence of the amplitudes from the regularly timed events.

DOI: 10.1103/PhysRevE.92.052904 PACS number(s): 05.45.Ac, 05.45.Xt

I. INTRODUCTION

The characterization of a dynamical system as *chaotic* suggests erratic, unpredictable evolution. However, it is well known that many chaotic oscillations have an approximately cyclic nature such that a phase can be defined similar to the phase of a sinusoidal oscillation [1]. Typically, the phase of a chaotic oscillator increases nearly steadily in time, but with small erratic fluctuations determined by initial conditions. For example, the phase of a Rossler oscillator has been modeled as a random walk superimposed on steady growth according to an average frequency [2]. A remarkably different behavior was observed in an unusual hybrid dynamical system [3–8]. Unlike most chaotic systems, an analytic expression is known for typical chaotic solutions of this hybrid system. Remarkably, each such solution must pass through points with zero slope at regularly spaced time intervals. These extrema and inflection points constitute a set of regularly timed events that occur amid an irregular chaotic oscillation. This phenomenon is striking since strict regular timing is a property one associates more with periodic systems (e.g., clocks) than with autonomous chaotic oscillators.

In this paper, we demonstrate that this phenomenon is general to a larger class of oscillators and has some interesting consequences. First, we identify the dynamic origin of regular events amid chaos, showing explicitly that they occur in all members of a class of solvable hybrid chaotic systems. Second, we show how a clock signal can be derived from the regular extrema and inflection points of a wave form generated by an electronic circuit that implements a solvable chaotic system. By making one parameter of the chaotic circuit adjustable, we introduce a feedback loop that phase locks the regular events in the chaotic wave form to an external periodic source. Next, a variation on this feedback scheme is used to produce a novel form of synchronization between two such chaotic circuits where their amplitudes are independent but their regular events coincide. Finally, we add an additional amplitude-dependent coupling that induces complete synchronization. However, we reverse the roles of drive and response in the second coupling to highlight the independence of the regular timing and the amplitude in the dynamics.

Solvable chaotic oscillators of the class considered here have a number of properties that make them fundamentally interesting as dynamical systems. For example, quantities such as the Lyapunov exponent and the metric entropy that are usually estimated statistically can be determined analytically. These oscillators may also have significant practical applications. Physical implementations include electronic circuits and electromechanical oscillators [3–5,7,9,10]. Proposed technological applications include radar [11–13] and communications [7,9,14–16]. Acoustic ranging using solvable chaos has been demonstrated experimentally [17]. In applications such as these, the presence of regularly timed events amid chaos enables easy integration of these oscillators into existing conventional, clocked, electronic technology and, therefore, may be the single most attractive feature of these dynamical systems from a practical standpoint.

II. A CLASS OF CHAOTIC OSCILLATORS WITH REGULAR EVENTS

A variety of hybrid oscillators with analytic chaotic solutions has appeared in the literature [3–8]. A general framework that incorporates all of these systems contains two components, as follows. The first component is the linear, second-order differential equation

$$\frac{d^2u}{dt^2} - 2\beta\frac{du}{dt} + (\omega^2 + \beta^2)(u - s) = 0, \tag{1}$$

where $u(t)$ is a continuous state variable, $s(t)$ is a discrete state, and ω and β are fixed parameters. The second component is a rule or *guard condition* that specifies how the discrete state $s(t)$ is updated. Here we consider the condition

$$\frac{du}{dt} = 0 \Rightarrow s(t) = H(u(t) - d), \tag{2}$$

meaning the discrete state $s(t)$ is set to $H(u(t) - d)$ whenever the derivative of $u(t)$ vanishes, where $H(x)$ is the

left-continuous Heaviside function and d is a fixed threshold. Various choices of the parameters ω, β, and d lead to the different solvable chaotic oscillators reported in the literature. For example, $\omega = 2\pi$, $\beta = \ln 2$, and $d = 1/2$ give an oscillator with a Lorenz-like phase portrait whose return map is exactly equivalent to the Bernoulli shift map. Also, $\omega = 2\pi$, $\beta = 0.81 \ln 2$, and $d = 1$ give an oscillator with a Rossler-like, folded-band phase portrait. These two examples illustrate how different choices for these three parameters may lead to topologically distinct chaotic sets in phase space. However, we show that, regardless of topological diversity, all such oscillators display regularly timed events in their chaotic solutions.

All oscillatory solutions of Eq. (1), a linear ordinary differential equation, have regularly spaced extrema or inflection points separated in time by half the natural period of oscillation. The guard condition Eq. (2) can only be triggered at such points. Importantly, the switching occurs in such a way that it does nothing to either hasten or delay the next such event. Thus, the set of regular events occurs in the full nonlinear system formed by Eqs. (1) and (2) through an interplay of the linear part and the discrete switching, as we will now show explicitly.

Consider an initial condition at time t_0 where $u(t_0) = u_0$, $du/dt(t_0) = 0$, and $s(t_0) = s_0 = H(u_0 - d)$. From $t = t_0$ until $t = t_1$, where t_1 is the next time at which $du/dt = 0$ and the guard condition is triggered, the solution is

$$u(t) = s_0 + (u_0 - s_0)e^{\beta(t-t_0)} \times \left(\cos\omega(t-t_0) - \frac{\beta}{\omega}\sin\omega(t-t_0)\right).$$

As long as this solution is valid, the derivative is

$$\frac{du}{dt}(t) = -\frac{\omega^2+\beta^2}{\omega}(u_0 - s_0)e^{\beta(t-t_0)}\sin\omega(t-t_0). \quad (3)$$

From Eq. (3) it follows that the next time at which $du/dt = 0$ is $t_1 = t_0 + \pi/\omega$. This argument can then be repeated using the initial condition at time t_1 where $u(t_1) = u_1$, $du/dt(t_1) = 0$, and $s(t_1) = s_1 = H(u_1 - d)$, to arrive at the conclusion that the next extremum or inflection point occurs at time $t_2 = t_1 + \pi/\omega$, regardless of whether $s_0 = s_1$ or not. Thus, starting from one extremum or inflection point of $u(t)$, there is an infinite train of extrema or inflection points at regularly spaced intervals of width π/ω. These points constitute a set of regularly timed events amid chaos.

Figure 1 shows chaotic solutions (solid black lines) of two hybrid oscillators. The first [shown in Fig. 1(a)] bears some resemblance to a Rossler oscillation insofar as it displays a sinusoidal oscillation that grows exponentially until it is folded back in by nonlinearity. The second [see Fig. 1(b)] is more like the antipodal Lorenz-type oscillation which has two growing oscillations about symmetric fixed points that are limited by jumping from one to the other rather than by a folding action. Despite the topological differences of these oscillations, both exhibit regularly occurring extrema and inflection points (indicated by red circles with dashed drop lines to underscore regular spacing in time). We emphasize that this phenomenon is generic to all the solvable systems that fit within the framework of Eqs. (1) and (2). Having established the generality of this phenomenon, in the following sections we describe experiments with chaotic electronic circuits that illustrate some consequences of regularly timed events amid chaos.

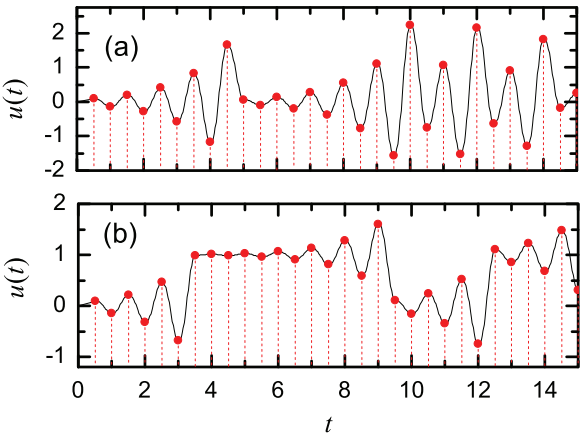

FIG. 1. (Color online) Time series of two solvable chaotic oscillators with extrema and inflection points highlighted (red circles). In both cases, $\omega = 2\pi$. The other parameters of the two oscillators are (a) $\beta = 0.7019$ and $d = 1.2632$ and (b) $\beta = 0.7645$ and $d = 0.5344$. Dashed guidelines indicate the regular spacing between the highlighted points.

III. A PERFECT CLOCK DERIVED FROM CHAOS

Oscillators governed by Eqs. (1) and (2) have been physically implemented as electronic circuits and electromechanical systems [3–5,7,9,10]. For any one of these devices, additional circuitry can be implemented to track the regularly timed events. Ideally, such a clock would be perfectly periodic with a period of exactly π/ω. Previously, a clock signal was derived from a Lorenz-like, antipodal chaotic wave form [17]. The approach used there cannot not be applied to all oscillators of the class considered here; specifically, it fails for those whose solutions contain a Rossler-like folding mechanism such as that shown in Fig. 1(b). Therefore, we now describe an electronic circuit with Rossler-like dynamics and a means for deriving a clock signal from the regularly timed events in the wave form. Some combination of this approach with that of Ref. [17] should suffice for any member of the class of oscillators considered in Sec. II.

The oscillator circuit, shown in Fig. 2, follows the same design as previously published solvable oscillators consisting of an analog resistor-capacitor-inductor circuit interfaced through comparators and buffers with a digital logic feedback circuit. The analog part implements the ordinary differential equation, Eq. (1), and the comparators, logic gates, and buffers implement the guard condition, Eq. (2). The continuous state variable $u(t)$ is proportional to the voltage $V_u(t)$ across the capacitor, C. A constant voltage V_d is supplied to set the threshold d. The discrete state variable $s(t)$ is proportional to $V_s(t)$, the output of the logic circuit which feeds back through the inductor L. The resistor $-R$ is an active negative resistance device. Extensive further details of the circuit implementation are given in the Supplemental Material [18].

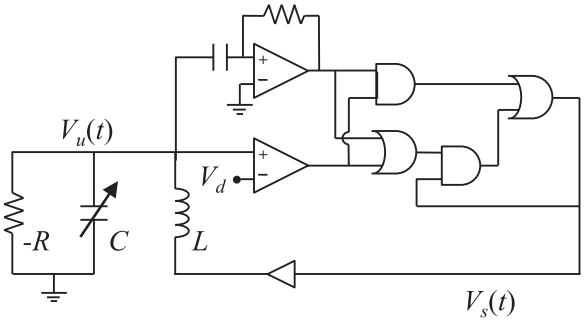

FIG. 2. Schematic diagram of a solvable chaotic oscillator circuit. A more detailed schematic is included in the Supplemental Material [18].

Typical behavior of the circuit is represented in Fig. 3. Figure 3(a) shows an experimental time series of the voltage $V_u(t)$ measured across the capacitor C. This oscillation resembles the Rossler oscillation insofar as it displays a growing sinusoid that is reinjected near the origin when it reaches a threshold size [19]. Figure 3(b) shows the corresponding phase portrait for this oscillator, where the voltage is plotted versus its derivative. Note that the phase portrait displays a folded-band structure similar to the oscillator in Ref. [8], but with the central eye opened considerably.

The regular events embedded in an oscillation like that of Fig. 3(a) are monitored with the simple circuit shown in Fig. 4 consisting of a comparator, a binary counter, and an XOR gate. To explain the function of the circuit, we refer to Fig. 5. A typical chaotic oscillation in $V_u(t)$ is shown in Fig. 5(a) and the corresponding discrete state V_s is shown in Fig. 5(b). The voltage V_s is supplied to the clock input of the binary counter. The output of the counter is a signal whose logic level switches on every falling edge of V_s, as shown in Fig. 5(c). The comparator outputs a logic signal whose state indicates the sign of the derivative of $V_u(t)$, with a low logic level indicating

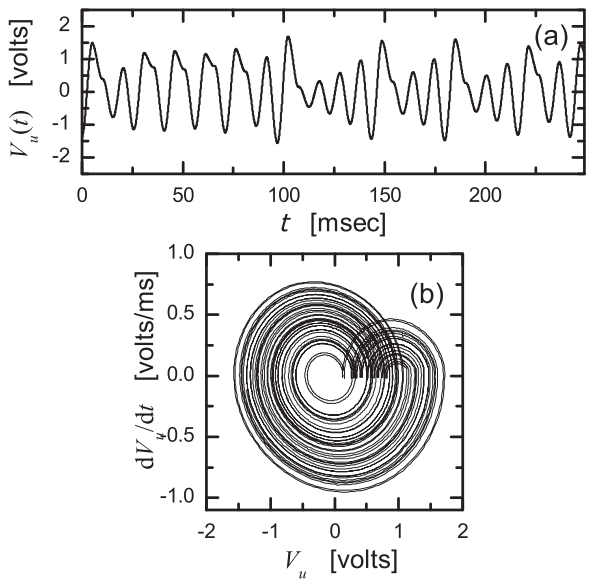

FIG. 3. Typical experimental (a) time series and (b) phase portrait of an electronic solvable chaotic oscillator.

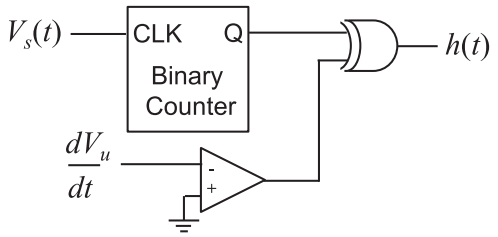

FIG. 4. Schematic diagram of a circuit that derives a periodic signal from the regular events found in the oscillations of the circuit of Fig. 2. Further circuit details are included in the Supplemental Material [18].

a positive sign, as shown in Fig. 5(d). This signal is a regular square wave whose polarity is flipped every time the guard condition triggers a rising edge in the discrete state $V_s(t)$. The XOR gate acts as either a logical follower or an inverter of this square wave depending on the input from the T flip flop. When the guard condition triggers a transition in $V_s(t)$, the polarity of the square wave at the output of the comparator is flipped, but the XOR gate flips it back, making the output $h(t)$ a regular square wave with a transition at each extrema or inflection point of the voltage over the capacitor, as seen in Fig. 5(e).

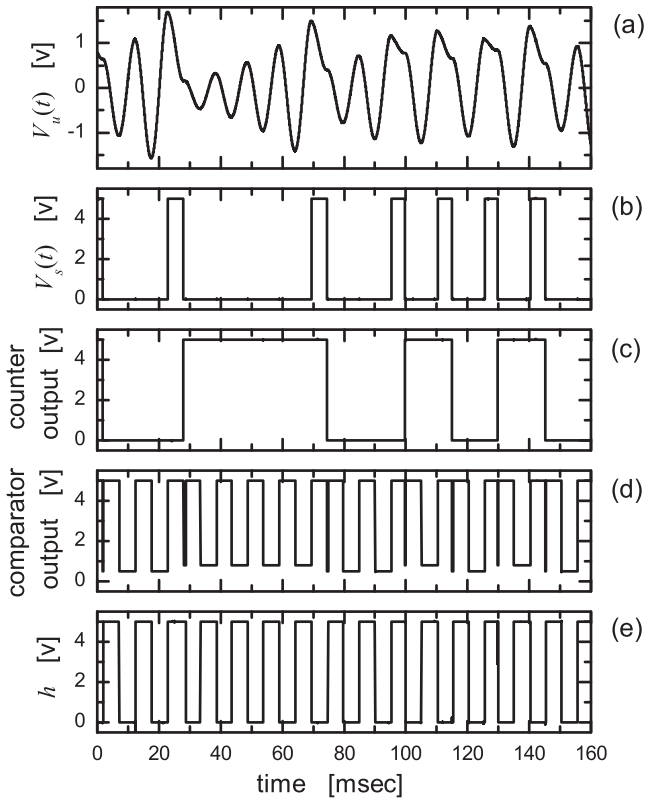

FIG. 5. Experimental data showing signals involved in deriving a periodic signal using the circuit of Fig. 4 from the regular events in the chaotic oscillations of the circuit of Fig. 2. Time series shown include (a) a chaotic time series with regular events, (b) the corresponding discrete state, and (e) the resulting periodic signal. The remaining time series [panels (c) and (d)] are intermediate steps corresponding to components in Fig. 4.

This circuit for extracting the regular timing of the oscillator in Fig. 2 can be compared with the similar circuit in Fig. 3 of Ref. [17]. The significant difference between these two circuits is the use here of a binary counter. The function of the counter is essentially to track the phase slips that occur each time the oscillation traverses the fold in the attractor seen in Fig. 3. No such folding or phase slips occur in the Lorenz-like attractor of Ref. [17], so no counter is needed. Thus, although regularly timed events are generic to a large class of solvable systems, the method of extracting them must take into account the specific topology of the attractor of interest.

Having established a means of extracting the regular timing of the chaotic signal, we can now contemplate exploiting it to modify the behavior of the chaotic oscillator in a desirable fashion. We describe two examples of such efforts below.

IV. PHASE LOCKING REGULAR EVENTS

In the previous section, a periodic signal was derived from the regular events in a chaotic oscillation. In many oscillator applications, it is useful to entrain one periodic oscillator to another. For example, in an FM receiver a local oscillator is phase locked to a received oscillation to enable demodulation. Here we show that the regular timing of a chaotic oscillation can likewise be entrained or phase locked. We first modify the oscillator circuit shown in Fig. 2 to enable small adjustments of the frequency of the regular events. Then we use the difference between the signal derived from the regular events and a reference signal to form a feedback control signal that adjusts the frequency of events in a manner that entrains or phase locks it to the reference signal.

Following the argument of Sec. II, the frequency of the regular events generated by Eqs. (1) and (2) is determined by the parameter ω. In our circuit implementation, this parameter is set primarily by the values of the capacitance C and the inductance L in Fig. 2. The capacitance C can be made variable by adding an electronically tunable capacitance in parallel with the existing fixed capacitance. The details of such a tunable capacitance are given in the Supplemental Material [18].

The voltage input that tunes the variable capacitance is used to feedback a control signal $g(t)$ related to the difference between the signal $h(t)$ derived from the regular events of the chaotic oscillator and a periodic reference signal $e(t)$. This scheme is illustrated schematically in Fig. 6. This feedback circuit has two inputs. The first is $h(t)$, the output of the circuit shown in Fig. 4. The second is $e(t)$, the reference signal whose

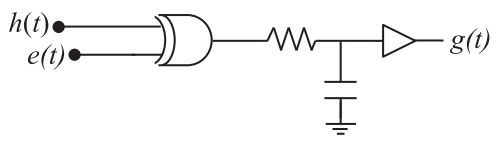

FIG. 6. Schematic diagram of a feedback circuit that locks the periodic signal $h(t)$ output by the circuit of Fig. 4 to an external signal $e(t)$. The output of this circuit $g(t)$ controls that variable capacitance in Fig. 2. Further circuit details are included in the Supplemental Material [18].

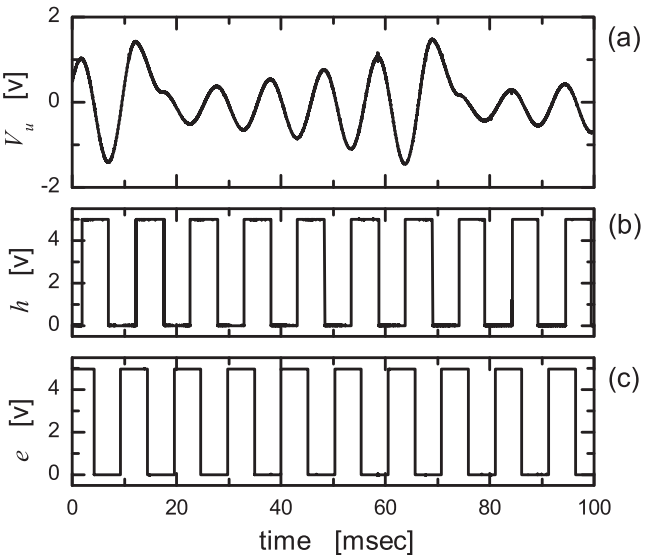

FIG. 7. Experimental time series demonstrating phase locking of (b) the periodic signal derived from the regular events in (a) a chaotic oscillation to (c) an external signal. In the locked state, a constant $\pi/2$ phase difference is apparent between the regular events and the external signal.

frequency is close to ω/π. The XOR gate and low pass filter then produce an output signal that is minimized when the two input signals have the same frequency and differ in phase by $\pi/2$ radians.

Figure 7 shows typical experimental examples of each of these signals. The consistent $\pi/2$ phase difference between the timing signal $h(t)$ and the reference signal $e(t)$ [shown in Figs. 7(b) and 7(c), respectively] is the hallmark of phase locking. It is important to note that the phase of the chaotic oscillation of the voltage $V_u(t)$ is not locked to the external signal as there is a π phase shift every time the oscillation goes through a fold [e.g., as occurs about 15 ms into the wave form of Fig. 7(a)]. However, apart from these instantaneous phase slips, the phase of the chaotic oscillation is governed by the external signal. Meanwhile, the chaotic oscillation of the voltage $V_u(t)$ continues unchanged. A detailed study of the transition to phase locking is beyond the scope of this article. However, we generally observed that the range of drive frequencies over which locking occurs increases with increasing feedback gain in a manner similar to other forms of phase locking.

Phase locking in one form or another is ubiquitous in modern communication technology. Thus, the demonstration of phase locking here suggests a degree of compatibility with conventional signal generation or processing schemes. This example of phase locking is directly applicable to a recently proposed scheme for generating antipodal chaotic wave forms for transmission of information [20]. In this scheme, the timing of a bank of solvable chaotic oscillators is assumed to be phase locked while the amplitudes are controlled to generate antipodal signals that are better suited for transmission and reception than the signal from an individual oscillator. This scheme was proposed without details on how to achieve phase

locking. Our results here provide a means of phase locking suitable to enable this scheme.

V. SYNCHRONIZATION OF REGULAR EVENTS

Phase locking is a particular example of the more general phenomenon of synchronization. Countless forms of synchronization have been observed in recent decades under a myriad of different coupling schemes. Many of these approaches are presumably applicable to solvable chaotic systems. Here we consider two particular coupling schemes that together highlight the significant degree of independence between the chaotic oscillation and its regularly timed events.

We first consider two identical solvable oscillators whose timing signals are coupled while their chaotic amplitudes are left free running. The coupling is implemented by using the timing signal of a free running solvable chaotic oscillator circuit in place of the external signal in Fig. 6. In this manner, the regular events of one chaotic oscillator are phase locked to the regular events of another.

Typical experimental time series of the coupled system are shown in Fig. 8. The continuous states of the drive and response oscillators, V_1 and V_2, respectively, exhibit a high degree of independence from each other, as seen in Figs. 8(a) and 8(b). This independence is even more apparent when V_1 is plotted versus V_2 as in Fig. 9(a). However, close inspection reveals a constant lag between the extrema and the inflection

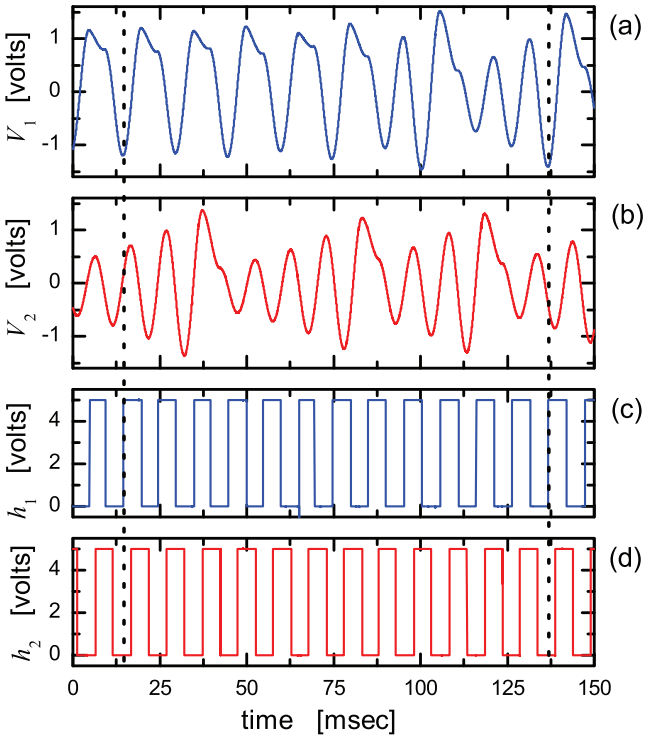

FIG. 8. (Color online) Experimental time series showing synchronization of regular events. (a) A first chaotic circuit oscillates freely. (b) A second chaotic oscillator evolves independently except with regular events occurring in step with those of the first oscillator (apart from a $\pi/2$ phase shift). Phase locking is apparent in the time series of the periodic signals [panels (c) and (d)] derived from each chaotic oscillator.

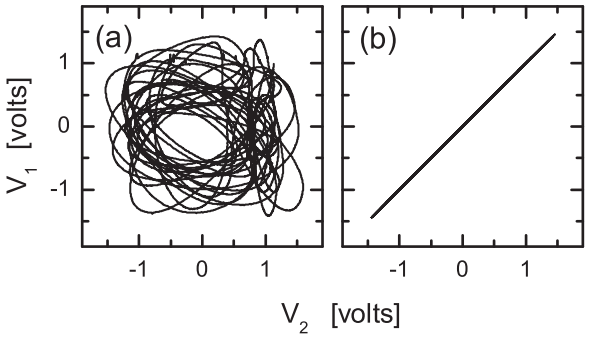

FIG. 9. Plots of one chaotic oscillation versus another in cases where (a) regular events are phased locked but no amplitude coupling is present and (b) both regular events and amplitudes are coupled.

points of V_1 and those of V_2. This synchronization of the timing signals, h_1 and h_2, is immediately apparent in Fig. 8. It is important to recognize that this state of synchronization does not exactly fit the definition of any previously reported form of chaos synchronization. It most closely resembles phase synchronization; however, the phases of the chaotic oscillations are not strictly locked as a phase shift of precisely π radians occurs every time either one of the oscillations goes through a fold.

Another interesting state of synchronization occurs when the timing signals of two solvable oscillators are locked and an additional unidirectional coupling is added proportional to the difference $V_1 - V_2$. The $\pi/2$ phase shift between the locked timing signals in Figs. 8(c) and 8(d) poses a difficulty to such a scheme since the regular events of the two oscillations do not coincide. In order to make the regular events coincide exactly, we introduce a binary counter before each input of the feedback circuit, as shown in Fig. 10(a). These counters reduce the frequency of timing oscillation by a factor of 2. Then a $\pi/2$ phase shift at this reduced frequency is equivalent to a π phase shift at the original frequency which is sufficient to make the regular events coincide. Then proportional feedback is easily introduced between the continuous states of the two

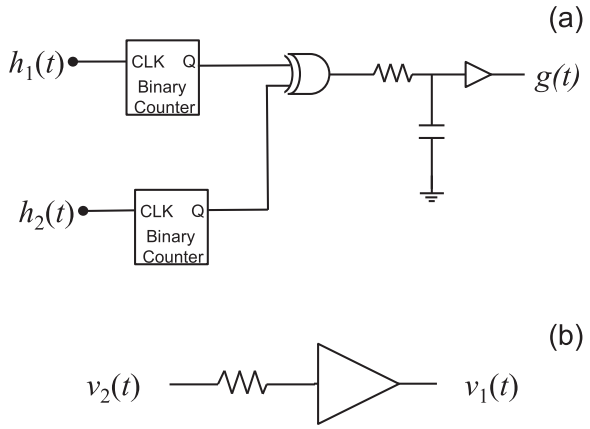

FIG. 10. Circuits for coupling (a) the periodic signals derived from regular events and (b) voltages corresponding to the continuous states of two chaotic oscillator circuits. Further circuit details are included in the Supplemental Material [18].

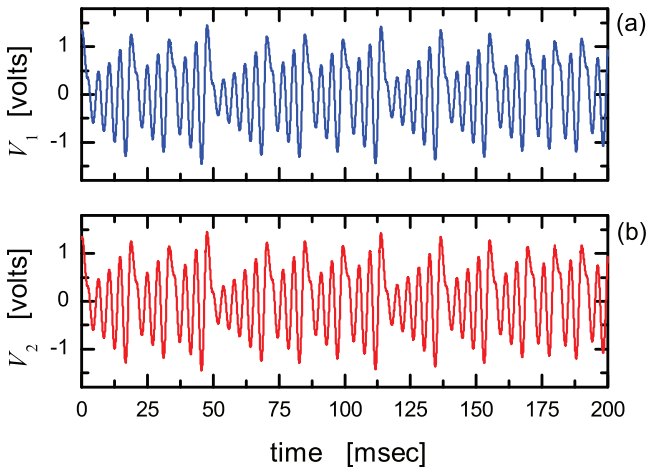

FIG. 11. (Color online) Time series of completely synchronized chaotic oscillations from two circuits under the coupling shown in Fig. 10.

circuits, V_1 and V_2, as shown in Fig. 10(b). Interestingly, due to the relative independence between the continuous state of the oscillator and its timing signal, this second coupling can be implemented in either the same direction as the phase locking, or in the opposite direction. Either configuration allows a state of identical synchronization. Figure 11 shows typical experimental time series for the system when the timing coupling is in the direction opposite that of the coupling of the continuous states. The continuous states of both oscillators, V_1 and V_2, shown in Figs. 11(a) and 11(b), respectively, follow identical trajectories with simultaneous regular events. Figure 9(b), showing V_1 plotted versus V_2, confirms the exact synchronization of the oscillators.

VI. CONCLUSION

In this paper, we have shown that the solutions of a topologically diverse class of chaotic oscillators are characterized by regularly timed events in which the derivative of the solution is zero. The perfectly periodic timing of these events is unexpected in light of the well-known unpredictability of chaos. We explored some consequences of these regularly timed events through experiments using chaotic electronic circuits. First, we showed that a feedback loop can be implemented to phase lock the regularly timed events to a periodic external signal. In this arrangement the external signal regulates the timing of the chaotic signal but does not lock its phase; only the phase of the regular events is locked. Second, we couple the regularly timed events of one chaotic oscillator to those of another. A state of synchronization is observed where the oscillators exhibit synchronized regular events while their chaotic amplitudes and phases evolve independently. Finally, we add additional coupling to synchronize the amplitudes as well, however in the opposite direction, illustrating the independence of the amplitudes from the regularly timed events. Regular timing is a common feature of most modern electronic systems. The ability of solvable chaotic systems to easily accommodate an external clock is likely to be a clear advantage over more typical chaotic systems in technological applications.

[1] A. Pikovsky, M. Rosenblum, and J. Kurths, *Synchronization: A Universal Concept in Nonlinear Sciences* (Cambridge University Press, Cambridge, UK, 2001).

[2] A. Pikovsky, M. Rosenblum, G. V. Osipov, and J. Kurths, Phys. D (Amsterdam, Neth.) **104**, 219 (1997).

[3] T. Saito and H. Fujita, Electron. Commun. Jpn. 1 **64**, 9 (1981).

[4] T. Tsubone, K. Mitsubori, and T. Saito, in *IEEE International Symposium on Circuits and Systems, 1996, ISCAS '96, Connecting the World* (IEEE, Atlanta, GA, 1996), Vol. 3, pp. 257–260.

[5] T. Tsubone and T. Saito, IEEE Tran. Circuits Syst, I: Fundam. Theory Appl. **45**, 172 (1998).

[6] N. J. Corron, Dyn. Contin. Discrete Impulsive Syst. A **16**, 777 (2009).

[7] N. J. Corron, J. N. Blakely, and M. T. Stahl, Chaos **20**, 023123 (2010).

[8] N. J. Corron and J. N. Blakely, Chaos **22**, 023113 (2012).

[9] A. N. Beal, J. P. Bailey, S. A. Hale, R. N. Dean, M. Hamilton, J. K. Tugnait, D. W. Hahs, and N. J. Corron, in *Proceedings of the 2012 Military Communications Conference, Orlando, FL, Oct. 29–Nov. 1, 2012* (IEEE, Orlando, FL, 2012).

[10] B. A. M. Owens, N. J. Corron, M. T. Stahl, J. N. Blakely, and L. Illing, Chaos **23**, 033109 (2013).

[11] J. N. Blakely and N. J. Corron, in *Proceedings of SPIE on Radar Sensor Technology XV*, Vol. 8021 (SPIE, Orlando, FL, 2011), p. 80211H.

[12] S. Zhang, J. Hu, and Z. He, in *Radar Conference 2013, IET International* (Institution of Engineering and Technology, 2013), p. 0179.

[13] L. Sun, J. Hu, C. Luo, and Z. He, in *Proceedings of the Second International Conference on Communications, Signal Processing, and Systems* (Springer, New York, 2014), pp. 541–548.

[14] N. J. Corron and J. N. Blakely, in *Proceedings of the Third IFAC CHAOS Conference* (International Federation of Automatic Control, Cancun, Mexico, 2012), pp. 19–24.

[15] J. N. Blakely, D. W. Hahs, and N. J. Corron, Phys. D (Amsterdam, Neth. (2013)) **263**, 99 (2013).

[16] H.-P. Ren, M. S. Baptista, and C. Grebogi, Phys. Rev. Lett. **110**, 184101 (2013).

[17] N. J. Corron, M. T. Stahl, and J. N. Blakely, Chaos **23**, 023119 (2013).

[18] See Supplemental Material at http://link.aps.org/supplemental/10.1103/PhysRevE.92.052904 for implementation details of all circuits.

[19] O. E. Rossler, Phys. Lett. A **57**, 397 (1976).

[20] D. W. Hahs, N. J. Corron, and J. N. Blakely, J. Franklin Inst. **351**, 2562 (2014).